Eur. Phys. J. B **25**, 431–438 (2002)
DOI: 10.1140/epjb/e20020049

THE EUROPEAN PHYSICAL JOURNAL B
EDP Sciences

Polarization-flip transition under electric field in BCCD

M. Quilichini[1,a], J.M. Perez-Mato[2], I. Aramburu[3], and O. Hernandez[4]

[1] Laboratoire Léon Brillouin, CEA de Saclay, 91191 Gif-sur-Yvette, France
[2] Departamento de Física de la Matería Condensada, Facultad de Ciencias, Universidad del País Vasco, Apdo. 644, 48013 Bilbao, Spain
[3] Departamento de Física Aplicada I, ETSIIT, Universidad del País Vasco, Apdo. 644, 48013 Bilbao, Spain
[4] UMR 6511 du CNRS-Université de Rennes 1, Institut de Chimie de Rennes, Bâtiment 10B, Campus Beaulieu, Avenue du Général Leclerc, 35042 Rennes, France

Received 20 September 2001

Abstract. Three-axes elastic neutron scattering measurements demonstrate that the five-fold modulated phase (phase 1/5) of BCCD exhibits under electric field a phase transition without change of superlattice periodicity. Through the monitoring of high-order satellite diffraction peaks as a function of electric field and temperature, the competition between this phase and neighboring polar phases with other periods has been characterized. At a threshold electric field of about 20 kV/cm, a rather abrupt redistribution of the satellite intensities of phase 1/5 is observed, without change of the corresponding primary modulation wave vector ($\frac{1}{5}\mathbf{c}^*$). A quantitative analysis of these intensity variations confirms the earlier conjecture based on dielectric experiments that the modulation essentially changes from a non-polar sequence 5up5down ($\langle 5 \rangle$) of polarized z-perpendicular layers of basic semicells, to a polar sequence 6up4down ($\langle 64 \rangle$). The transition is caused by the *flip* of the average polarization of one of the interface layers, and can then be described as a bounded discrete motion of the *wall* separating positive and negative microdomains within the five-fold unit cell. This type of polarization-flip phase transition had been detected and characterized in one-dimensional theoretical models as generalized Frenkel-Kontorova models or spin chains with elastic couplings, but had not been anticipated in theoretical analyses of BCCD, for which other phenomenological or microscopic models (as the ANNNI model) have been considered adequate. Only recently and in view of the experimental results reported here, we demonstrated, using a general phenomenological displacive model, the possibility of this type of transition in systems as BCCD [Phys. Rev. B **62**, 11418 (2000)]. Phase diagrams with spin-flip phase transitions yield very peculiar phase diagrams with a checkerboard topological structure and self-similar features. In particular, they may present special critical points as the so-called *upsilon* points [J. Statistical Phys. **62**, 45 (1991)]. BCCD may be then the first experimental system where they could be observed.

PACS. 64.70.-p Specific phase transitions

1 Introduction

Solids with an incommensurate structural thermal instability can exhibit complex phase sequences as a function of temperature with several intermediate commensurate phases where the structural modulation locks into different multiple periodicities of the underlying basic lattice. BCCD (Betaine Calcium Chloride Dihydrate, $(CH_3)_3NCH_2COO.CaCl_2.2H_2O$) is the most conspicuous experimental case with more than fifteen intermediate commensurate phases of different periods detected between room temperature and 0 K, so it has been considered as the physical realization of the so-called incomplete devil'staircase [1,2]. At room temperature BCCD stabilizes in an orthorhombic Pnma paraelectric crystalline phase. Below $T_i = 164$ K the structural modulation develops with a wavevector $\mathbf{q} = \delta(T)\mathbf{c}^*$ with $q = \delta(T)(\frac{2\pi}{c_0}), (0 \leq \delta \leq 0.319)$. The lattice constant in the z direction is $c_0 = 10.824$ Å. For $T \leq 115$ K a harmless devil's staircase is observed as a series of commensurate phases $\delta = \frac{1}{4}, \frac{1}{5}, \frac{1}{6}$.... which stabilize successively with decreasing T. At $T_0 = 46$ K the compound reaches a non-modulated ferroelectric low temperature phase of $Pn2_1a$ symmetry, *i.e.* with the spontaneous polarization along the b-axis. According to the symmetry of the structural modulation or to the order parameter, the polarity of the different intermediate modulated phases only depends on the parity of the fraction δ. Phases with $\delta = \frac{odd}{odd}$ are non polar phases, while those with $\delta = \frac{odd}{even}$ are polar along

[a] e-mail: kilik@llb.saclay.cea.fr

the a-axis. Only phases with $\delta = \frac{even}{odd}$ are polar along the b-axis, as the final ferroelectric $\delta = 0$ phase [3].

The type of phase diagrams with several competing commensurate and incommensurate periodicities observed in BCCD can be somehow simulated with spin lattice models generalized to include competing interactions, as the ANNNI (axial next nearest neighbor Ising) model and its derivatives [4]. In fact, such phase diagrams are quite common among magnetic materials [5]. Within this simplified model, a pseudospin is associated to each semicell along the c-axis representing a local two-valued dielectric polarization along the b-axis; the structural modulation is then reduced to the configuration of a 3D pseudospin system. Under this scheme, the ANNNI model has been quite successful in reproducing many features observed in BCCD, in particular its phase diagram as a function of hydrostatic pressure and temperature [6,7]. Assuming a saturated regime where the lattice planes perpendicular to the c-axis have all a saturated polarization, the modulation is effectively described by a one-dimensional chain of *"polar"* spins, whose net polarization (along the b-axis) is given directly by the spin configuration. For each phase δ, the equilibrium spin configuration at zero electric field is in general that with minimal net polarization compatible with the period and primary wavelength forced by the δ value. Hence, for phase 1/4 and 1/5, the spin modulations would be $\uparrow\uparrow\uparrow\uparrow\downarrow\downarrow\downarrow\downarrow$ and $\uparrow\uparrow\uparrow\uparrow\uparrow\downarrow\downarrow\downarrow\downarrow\downarrow$, respectively, or in short notation the configurations $\langle 4\rangle$ and $\langle 5\rangle$, which are non-polar, while for phases 2/7 or 2/9, one expects the polar configurations $\uparrow\uparrow\uparrow\uparrow\downarrow\downarrow\downarrow$ and $\uparrow\uparrow\uparrow\uparrow\uparrow\downarrow\downarrow\downarrow\downarrow$, respectively, or in short $\langle 43\rangle$ and $\langle 54\rangle$. As emphasized above, one should note that the pseudospins in this notation refer to semicell along the c-axis. Thus, for example, the actual period of a configuration like $\langle 54\rangle$ is 5454 to complete a number pair of spins and semicells, and corresponds to a superstructure cell of parameter 9c, as it should be. This scheme explains in a simple manner the dependence of the b-polarity on the δ-parity. This picture, although quite reduccionist with respect to the actual experimental modulated structures observed in phases 1/4 and 1/5, contains an essential point which was indeed confirmed by the experimental structural analysis [8], namely, that the modulation is essentially saturated in phases 1/4 and 1/5, and for many atoms is approximately described along the b-axis by a step-like *"solitonic"* function.

The dependence with electric field (E) (along the b-axis) of the harmless phase diagram of BCCD has been previously investigated using diffraction experiments only at low fields in [9–11]. Le Maire *et al.* [12] arrived to propose a rather complete (E,T) phase diagram including higher fields up to about 20 kV/cm, from purely macroscopic dielectric measurements and using an inert gas small pressure to avoid dielectric breakdown. In general, as expected, the b-polar phases are favored by the field. Hence, the electric field reduces progressively the stability range of non-polar phases as 1/4 and 1/5, stabilizing instead the neighboring polar ones 2/7, 2/9 or 2/11. At higher fields, Le Maire *et al.* [12] reported an important new feature shown in Figure 1, where a scheme of

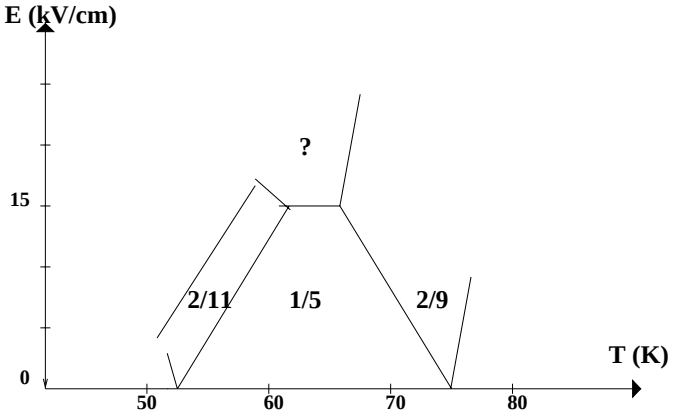

Fig. 1. Scheme of the (E,T) phase diagram of BCCD at low temperature proposed by Le Maire *et al.* [12].

their phase diagram in the temperature domain around phase 1/5 is approximately reproduced. At a threshold field of about 16 kV/cm, a new phase seems to stabilize and overcomes the competition with the neighboring phases 2/9 and 2/11, whose stability ranges start decreasing at the expense of the new phase. From the value of the saturated polarization of the hysteresis loops observed within this new phase, Le Maire *et al.* conjectured that the new phase should correspond to a local polarization flip. The system would pass from a $\langle 5\rangle$ configuration (5 spins up and 5 spins down) to a configuration $\langle 64\rangle$ through the "flip" of an interface pseudospin from negative to positive values. This transition could then be considered as a discrete sliding of the walls separating microdomains of positive and negative polarization. In phase 1/5 at low fields, these walls are regularly spaced along the c-axis separating domains of 5 semicells, the threshold field would unpin these walls through the polarization flip of a whole plane of semicells and would increase the positive microdomains to 6 semicells, reducing the negative ones to 4. In this sense, the effect of the electric field would be similar to the well-known domain switching in normal ferroelectrics through domain wall displacements. The important difference is that here the domains extend only a few cells along the modulation direction and form a coherent regular lattice, not fitting the usual continuous field approximation used for domain walls. In addition, the domain-wall displacements are also coherent, do not surpass the atomic scale and are constrained to a fixed discrete value.

The existence of this polarization-flip transition can be considered a logical consequence of the approach at higher fields of the temperature stability domains of phases 2/9 and 2/11. As the free energies of configurations $\langle 65\rangle$ and $\langle 54\rangle$ become similar, it seems natural to expect that configuration $\langle 64\rangle$, which would be realized at the interface of the two previous ones, will become competitive and finally overcome at higher fields due to its higher net polarization.

Despite being physically quite reasonable, this type of polarization-flip phase transition has never been observed in other modulated polar materials and, in general, has not been anticipated by theoretical models of

BCCD [10,13,14]. General studies of microscopic models with competitive interactions as the ANNNI or the DIFFOUR models, usually considered adequate to reproduce the main physics involved in BCCD, have also not reported such type of transitions in their phase diagram [4,15–21]. Phase diagrams of magnetic systems with various modulated magnetic phases such as CeSb or UPd_2Si_2 do not seem also to have such type of transition [5,21].

On the other hand, Aubry [22] predicted a phase diagram as a function of tensile force and field for a generalized Frenkel-Kontorova model which presents topological features similar to those observed in BCCD. In this phase diagram, phase transitions, which can be assimilated as a polarization-flip, are ubiquituous and systematic. According to this work, successive polarizations flips can take place as electric field increases producing a characteristic pattern in the phase diagram. Phase diagrams with similar topologies and systematic flip transitions have also been reported for a one-dimensional Ising chain with elastic coupling [23] and for a one-dimensional Ising chain with long-range interaction plus uniform and staggered fields [24]. But this type of phase diagrams is not restricted to spin-like or order-disorder systems and we recently showed that a phase diagram with similar features including polarization flip transition, can be realized in a displacive phenomenological model much closer to the mechanism involved of BCCD [25]. Using a soft-mode scheme similar to the one observed in BCCD [26], a generalized Landau-Ginzburg free-energy describing two anticrossed phonon branches, one of them thermally soft, was sufficient to produce at low temperatures step-like modulations, looking like a sequence of spins "up" and "down", which under the electric field exhibited polarization-flip transitions. Thus, it seems that these spin-flip transitions, despite earlier model calculations, should be a rather universal feature in modulated systems with competing periodicities along a single direction. Nevertheless, no experimental case, including magnetic systems, had been reported before Le Maire *et al.* [12]. Up to our knowledge, if confirmed, BCCD would be the first material where this feature is indeed observed.

The purpose of the present work is to ascertain and characterize with elastic neutron scattering data the (E,T) phase diagram of BCCD in the domain depicted by Figure 1. In particular, we pretend to confirm and analyze with a microscopic technique the polarization-flip transition of the structural modulation in phase 1/5, so far only proposed from the results of dielectric measurements.

2 Experimental

2.1 The sample

A single crystal of fully deuterated BCCD (DBCCD) was shaped as a platelet ($10 \times 5 \times 1.3$ mm^3). Gold electrodes were deposited in vacuum from a gold target onto the two rectangular faces normal to the b direction. The gold thickness of the electrodes was about 2000 Å. An electric voltage as high as 3 kV was applied to obtain a dc electric field parallel to the b axis of the structure. The thickness (1.3 mm) of the platelet was carefully checked in order to determine the electric field value and its homogeneity within the sample. The sample was glued on its holder and enclosed in an aluminum container with 20 bars of He gas. This box was mounted on the cold finger of a Displex closed-cycle cryostat. The temperature at the sample was stable within ± 0.05 K during a complete run.

2.2 The measurements

Elastic neutron scattering measurements were performed on a 4F three axis spectrometer located on the cold source of the Orphée reactor, Saclay, France. The scattering plane defined by the wave vectors $\mathbf{k_i}$ and $\mathbf{k_f}$ of the incident and outgoing neutron beams, respectively, was the ($\mathbf{b}^*$, $\mathbf{c}^*$) reciprocal plane of the crystal at room temperature (orthorhombic symmetry). The vectors $\mathbf{k_i}$, $\mathbf{k_f}$, $\mathbf{Q}$ with $\mathbf{k_i} - \mathbf{k_f} = \mathbf{Q} = \mathbf{G} + \mathbf{k}$ define the scattering geometry, with $\mathbf{Q}$ the transferred momentum during the scattering process and $\mathbf{G}$ a reciprocal vector of the basic lattice of main reflections. We have mainly recorded elastic scans with $\mathbf{k}$ along the c^* direction, *i.e.* $\mathbf{k} = \eta\mathbf{c}^*$, in order to detect the satellite reflections of the main reflection $G = (0\ 4\ 0)$ along the line $(0\ 4\ \eta)$. A compromise to work with a good resolution and signals which do not require too large measuring time was obtained with the following experimental conditions: $k_i = 1.55$ Å^{-1} from monochromator and collimations of 10 and 20 minutes before and after analyser, respectively. Both monochromator (vertically bent) and (flat)analyser are of pyrolitic graphite (PG[002]). Chosen values of k_i and k_f are obtained through Bragg reflection from a set of lattice planes on the monochromator and on the analyser, respectively. A beryllium filter cooled with liquid nitrogen was used to get rid of the second order contamination.

The data were collected only on cooling runs. Before each measurement the temperature was stabilized requiring about 20 to 30 minutes depending on the temperature step. The temperature step varied from 2 degrees to half a degree in the temperature range of interest. Elastic scans through second order and third order satellites were collected systematically and lasted about one hour. In some cases, also scans of the first order satellites were collected. The complete data collection at each electric field value lasted about 72–80 hours.

2.3 Data treatment

All raw collected data were fitted taking into account resolution effects of the spectrometer. Usually the best fit was obtained superposing Lorentzian functions for each observed diffraction peak. These functions have been used systematically during the whole data process. The background was constrained to have a constant value for equal measuring times. The normalized integrated intensity of the fitted Lorentzian was then identified with the intensity of the corresponding diffraction peak.

2.4 Experimental results

The temperature and electric field domains where we have concentrated our experimental effort correspond broadly to the part of the (E, T) phase diagram sketched in Figure 1. The scattering plane chosen for our elastic measurements corresponds to Bragg reflections $(0klm)$ in the usual 4-integer indexation of one-dimensionally modulated phases, where $\mathbf{Q}_{\mathrm{Bragg}} = h\mathbf{a}^* + k\mathbf{b}^* + l\mathbf{c}^* + m\mathbf{q}$. In the incommensurate phase and at zero field the reflections on this plane are extinct for $k + l = odd$, due to the operation $\{m_x|0, \frac{1}{2}, \frac{1}{2}, 0\}$ present in its superspace group $\mathrm{Pnma}(00\gamma)1s\bar{1}$. This is a fortunate situation that enables to monitor high-order satellites without overlapping problems with low-order ones associated to the nearest main reflection. Thus, as all reflections $(0\ 4\ 1\ m)$ are extinct (including the main reflection $m = 0$), the closest reflections to interfere with those of type $(0\ 4\ 0\ m)$ (with m positive) measured along the line $(0\ 4\ \eta)$ $(\eta \leq 1)$ are those associated to the main reflection $(0\ 4\ 2)$, *i.e.* satellites $(0\ 4\ 2\ m)$ with m negative. In the commensurate phases, indeed satellites are to superpose coherently, breaking in general the unambiguity of the 4-integer indexation. However, superspace group extinction rules are kept for the superposing reflections. Thus, for instance, in phase 1/5, the satellite reflection of third order $(0\ 4\ 0\ 3)$ located at $(0\ 4\ 0.6)$ does not suffer any overlap with the satellite of second order $(0\ 4\ 1\ -2)$ located at the same point, as this is extinct. Its first correction due to a coherent commensurate superposing will come from the seventh order satellite $(0\ 4\ 2\ -7)$, which can be neglected in a good approximation. Something similar happens for second and fourth order satellites where the first effective superposing will take place with eighth and sixth order satellites respectively. This favorable circumstance does not change when an electric field is applied along the b-axis. The field will in general break the superspace symmetry and reduce the symmetry, but the superspace symmetry operation causing the favorable extinction rule, being compatible with the field, is maintained.

Figure 2 presents a typical elastic scan $(0\ 4\ \eta)$ at $T = 64.4$ K and $E = 5$ kV/cm showing the second and third order satellites corresponding to phase 1/5. The temperature being at about the center of the stability range of this phase, the peaks can be observed isolated. In general, however, a persistent coexistence of the three competing phases was observed. Figure 3 depicts the form of these scans for an intermediate field of 10 kV/cm as a function of the temperature. The second and third order satellites located at the points corresponding to phase 1/5 coexist with the equivalent ones for phase 2/11 and phase 2/9 in the low and high temperature domains, respectively. These coexistence regions can be quite large and extend in general several kelvin. At higher fields, when the domain of phase 1/5 reduces to a few kelvin, the simultaneous coexistence of the three phases can be observed, as shown in Figure 4. In principle, this phase coexistence cannot be attributed in a significant part to temperature gradients, as these should have values well beyond any reasonable estimate. Therefore, its origin is probably a strong metastability of the competing phases and perhaps some uncontrolled inhomogeneity of the electric field. Similar strong coexistence of neighbouring phases was also observed in previous experiments at low electric fields [10,11]. This situation precludes a meaningful determination of the stability border lines of the different phases in the phase diagram. This contrasts with the dielectric measurements in [12], where the metastability of the phases, if existing, was no obstacle for observing well-defined borders between the phases. Nevertheless, we could obtain a rough estimation of the phase diagram by establishing, at each measured field, the temperature interval where phase 1/5 was majoritary as indicated by its

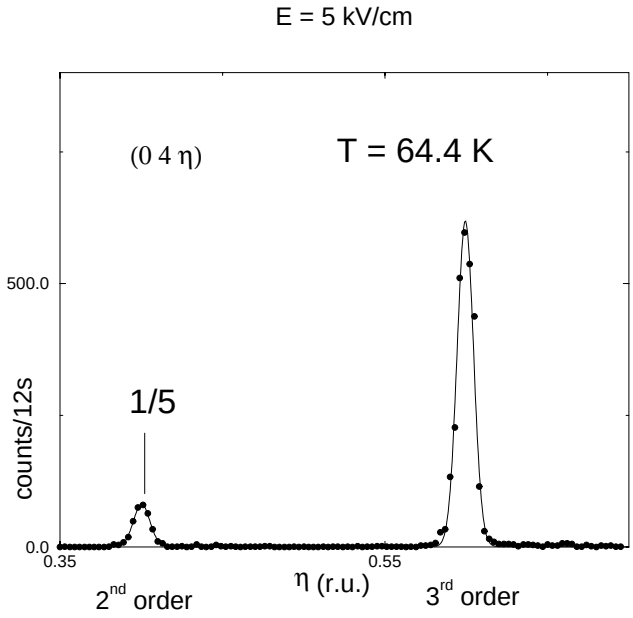

Fig. 2. Elastic scan obtained at $E = 5$ kV/cm and $T = 64.4$ K showing the second and third order satellites corresponding to phase 1/5.

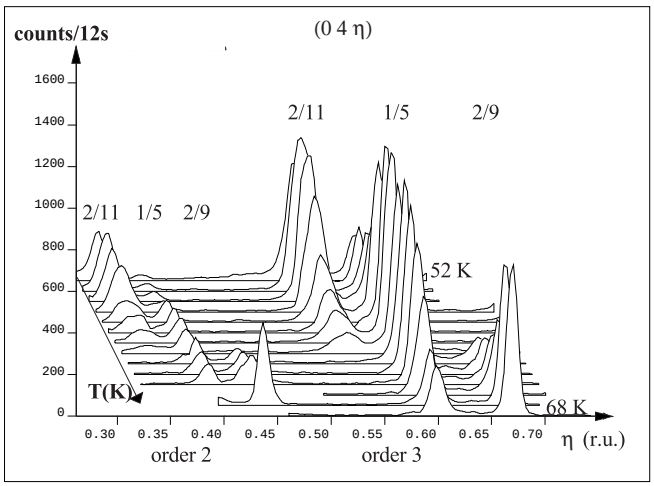

Fig. 3. Elastic scans at $E = 10$ kV/cm as a function of temperature from 52 K to 68 K, showing in general the coexistence of satellite peaks of phases 1/5, 2/9, and 2/11.

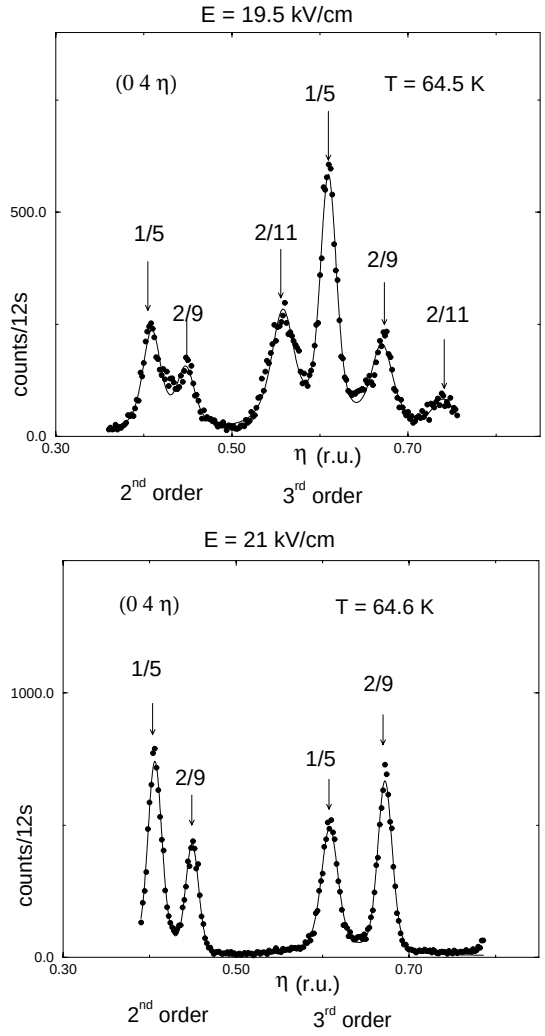

Fig. 4. Elastic scans at about 64.5 K for $E = 19.5$ kV/cm and 21 kV/cm showing the strong variation of the relative intensities of the second and third order satellites for phase 1/5.

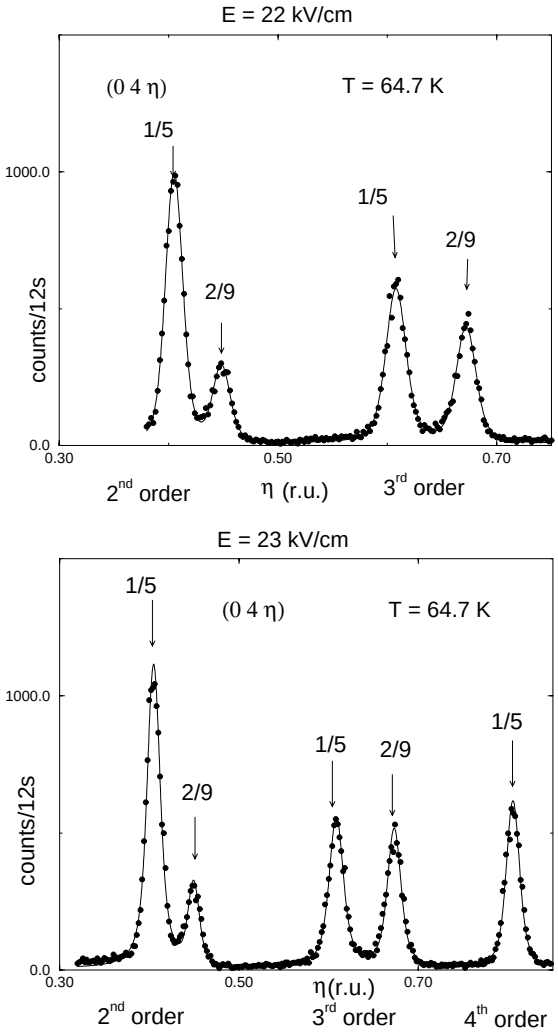

Fig. 5. Elastic scans at $E = 22$ kV/cm and 23 kV/cm. The new relative intensities of the second and third order satellites for phase 1/5 is stabilized. The strong intensity of the 4th order satellite is also shown at 23 kV/cm.

third order satellite having a higher intensity than those corresponding to any of the other two phases. Using this somehow arbitrary criterion, the phase diagram of [12] is confirmed in broad terms, but the field values involved is somehow larger. Normal phase 1/5 has an appreciable stability temperature range up to electric field values of the order of 20 kV/cm, while this reduces to about 16 kV/cm in the dielectric measurements.

The strong uncontrollable metastability of the different phases also precludes the establishment of a direct relation between the variation of the structure and the changes with temperature or electric field of satellite absolute intensities. Obviously, an important part of the intensity variations could be due to changes in the share of each competing phase within the sample. Only the ratios between the intensities of different satellites corresponding to the same phase are free from this effect and can be used to ascertain the structure evolution of the corresponding phase with temperature and electric field. Typically the intensity of the satellites of second order is much smaller than those of third order, while these latter are much weaker than the first order satellites. This is systematic for the three phases concerned (see Fig. 3). At 5 kV/cm the ratios for phase 1/5 of first and second order satellite intensities with respect to the corresponding third order satellite, henceforth called I_1/I_3 and I_2/I_3, were 7 and 0.1, respectively. For low electric fields, this ratio is quite insensitive to temperature and electric field changes. This must be related with the fact that the modulation is quite saturated in this temperature range, both in amplitude and step-like form and does not significantly vary. I_2/I_3 is somehow larger for phases 2/11 and 2/9, being typically of the order of 0.3 and 0.5, respectively. As the electric field raises, I_2/I_3 stays essentially constant for phases 2/9 and 2/11, while in the case of phase 1/5, an abrupt increase takes place between the two measurements done at 19.5 kV/cm and 21 kV/cm, as seen in Figure 4. I_2 clearly surpasses I_3 at 21 kV/cm, and I_2/I_3 is already about 2 at 22 kV/cm, while the following measurement performed at 23 kV/cm indicates that I_2/I_3 saturates (see Fig. 5). If measurements at different temperatures are compared, the

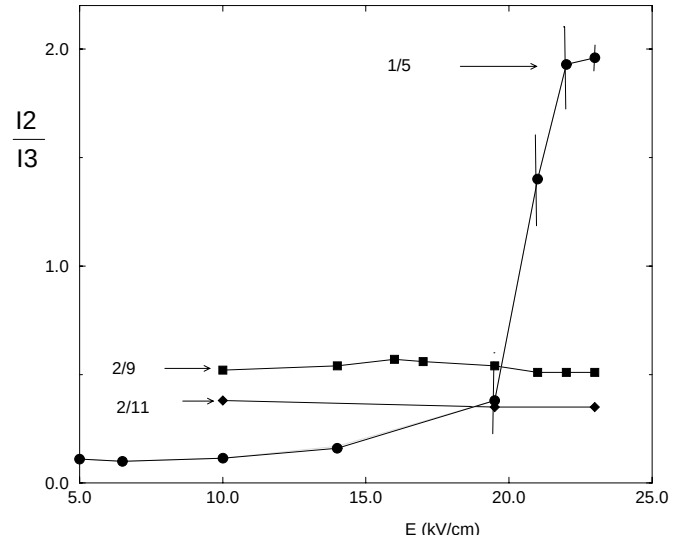

Fig. 6. Behaviour as a function of electric field of the ratio of the second and third order satellites I_2/I_3 for the three competing phases 1/5, 2/9 and 2/11. The points correspond to the average values obtained for different temperatures within the domain where the phase is clearly observed. Such a temperature domain (around 64.5 K) depends of the electric field value. An error bar corresponding to the standard deviation of these values is indicated when significant.

value of I_2/I_3 is essentially temperature independent for phases 2/9 and 2/11. This is also the case for phase 1/5 at low fields, but at fields 19–22 kV/cm I_2/I_3 has significant temperature variations, while it becomes again essentially temperature independent at 23 kV/cm. Measurements at higher electric fields were not done to avoid dielectric breakdown of the samples.

In Figure 6 a summary of the behaviour of I_2/I_3 for the different phases is depicted. The error bars in the figure correspond to the variations observed between scans at different temperatures mentioned above. Clearly, an abrupt redistribution of the satellite intensities for phase 1/5 takes place at about 21 kV/cm indicating a discontinuous change in the structural modulation, while keeping the value of the primary modulation wave vector. In accordance with the results of Le Maire *et al.* [12], we could observe that, beyond this threshold field, the stability temperature range of the new phase 1/5 spreads at the expense of the neighboring ones. The scan displayed in Figure 5 at 23 kV/cm shows that the intensity of the fourth order satellite of phase 1/5 has also become very strong, being comparable to I_3. In fact, the value of I_4/I_3 at 23 kV/cm, for all scans with a significant part of the new transformed phase 1/5, is about 1.0. The ratio I_1/I_3 also suffers a large jump changing from the value of 7 observed at low fields to 25.

3 The polarization-flip transition

The abrupt change at higher-fields of the satellite intensity ratios I_2/I_3 and I_4/I_3 of phase 1/5 reported and characterized in the preceding section can be demonstrated to be indeed the signature of a polarization-flip transition. As explained above, for the satellites actually measured in this work the commensurate coherent overlap of higher order satellites can be neglected in a good approximation. Hence, we can quantitatively argue as in the case of an incommensurate modulation despite the phase being commensurate. Obviating the thermal Debye-Waller factors, the intensity of a given satellite is proportional to the modulus of the corresponding structure factor:

$$F(\mathbf{H}) = \sum_j b_j \mathrm{e}^{\mathrm{i}\mathbf{H}\cdot\mathbf{r_j}} g_j^m(\mathbf{H}) \tag{1}$$

where $\mathbf{H}$ ($= \mathbf{Q}_{\mathrm{Bragg}}$) is the diffraction vector, b_j and $\mathbf{r_j}$ are the coherent scattering length and average position of atom j in the average unit cell. $g_j^m(\mathbf{H})$ can be considered as a form factor resulting from the modulation and is given by

$$g_j^m(\mathbf{H}) = \int_0^1 \mathrm{d}v \mathrm{e}^{\mathrm{i}(\mathbf{H}\cdot\mathbf{u}_j(v)+2\pi m v)} \tag{2}$$

where m is the satellite index of reflection $\mathbf{H}$ and $\mathbf{u}_j(v)$ is the displacive modulation function of atom j. These functions have been determined by neutron diffraction by Hernandez *et al.* [8] both for phases 1/4 and 1/5 . According to this work, the atomic modulation functions have soliton character and can be regarded as step-like functions (see Fig. 7). In a zeroth order approximation they can be expressed as [27]:

$$\mathbf{u}_j(v) = A(v)\mathbf{e}_j \tag{3}$$

where the set of vectors $\mathbf{e}_j$ constitutes a polar B_{2u} mode, while $A(v)$ is a step-like function ($A(v) = 1$, $\Delta > v \geq 0$; $A(v) = -1$, $1 > v \geq \Delta$; $\Delta = 1/2$). Approximating $\exp(\mathrm{i}\mathbf{H}\cdot\mathbf{u}_j(v))$ by $1 + \mathrm{i}\mathbf{H}\cdot\mathbf{u}_j(v)$, the form modulation factors $g_j^m(\mathbf{H})$ for satellites ($m \neq 0$) is proportional to the corresponding Fourier component of $\mathbf{u}_j(v)$, and therefore of $A(v)$. Thus, for satellites:

$$F(\mathbf{H}) = A_{-m}\left[\sum_j b_j(\mathrm{i}\mathbf{H}\cdot\mathbf{e_j})\mathrm{e}^{\mathrm{i}\mathbf{H}\cdot\mathbf{r_j}}\right] \tag{4}$$

with $A_{-m} = \int_0^1 \mathrm{d}v A(v)\mathrm{e}^{\mathrm{i}2\pi m v}$.

A polarization-flip transition implies in this picture a change of the Δ value of the global function $A(v)$ from 0.5 to 0.6, as schematized in Figure 8. This means, in practice, that the sixth atomic displacement in the atomic modulations depicted in Figure 7 for phase 1/5 should suffer a jump and acquire approximately opposite values. Neglecting the small difference of the satellite diffraction vectors, the variation of the satellite intensity ratio is then expected to be directly correlated with the variation of the ratio of the square moduli of the Fourier amplitudes $|\ A_m\ |^2 = \frac{4}{(n\pi)^2}\sin^2(n\pi\Delta)$. A shift of Δ from 0.5 to 0.6

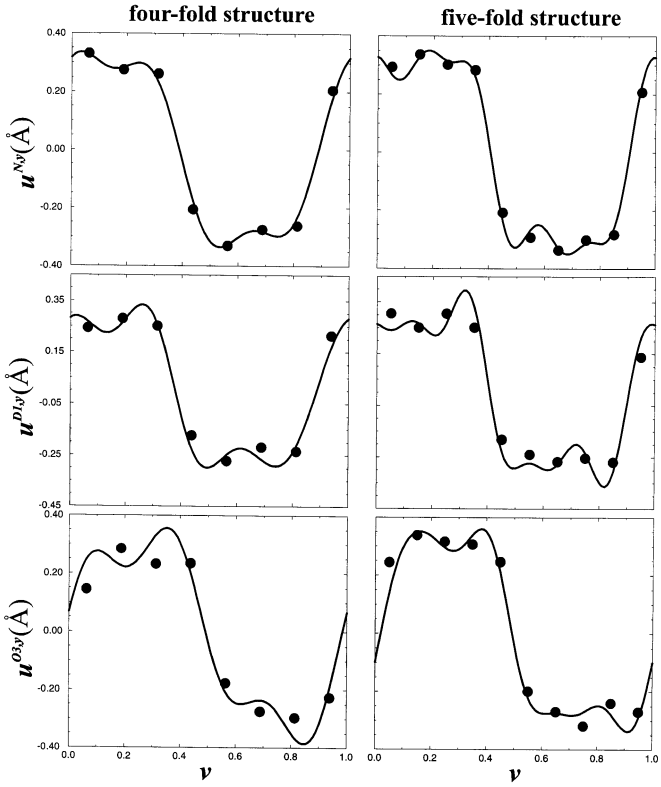

Fig. 7. Atomic modulations along the polar axes of atoms O_3, D_1 and N of BCCD in phases 1/4 and 1/5 [8]. The points describe the discrete atomic displacements obtained in a standard commensurate structure determination. Both approaches show the saturation of the modulation and its strong step-like form.

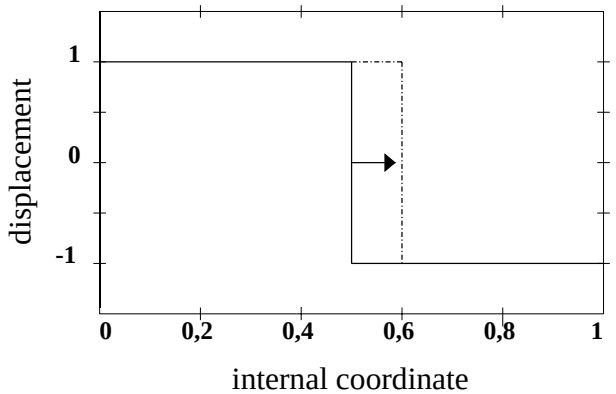

Fig. 8. Scheme of the change in the idealized modulation function $A(v)$ corresponding to the polarization-flip transition.

would then imply a variation of I_2/I_3 and I_4/I_3 from zero to values around 2.3 and 1.5, respectively. Something of this sort takes place indeed in DBCCD around 20 kV/cm. Although overestimated, these values roughly correspond to the abrupt observed increase of both ratios. One should note that $\mid A_m \mid^2/\mid A_n \mid^2$ is strongly dependent on Δ. Thus, for instance, $\mid A_2 \mid^2/\mid A_3 \mid^2$ would be 0.3, 60 and 21 for Δ= 0.55, 0.65 and 0.70, respectively, while the value of $\mid A_4 \mid^2/\mid A_3 \mid^2$ for the same Δ values would be 0.2, 20 and 2, respectively. Therefore, the observed intensity ratios after the transition fit nicely with a shift of δ from 0.5 to 0.6. A better agreement would not be reasonable given the approximations included in the above derivation. For instance, the above reasoning would mean a ratio $I_1/I_3 = 9$, to be compared with the experimental value of 7 observed at low fields. This gives an idea of the relative error of the approximation. On the other hand, this ratio would change to 24 after the polarization-flip, which agrees with the observed value (25). The truncation of the exponentials to the first two leading terms of its Taylor expansions also yield, in general, unrealistic zero values for I_2, I_4 and all even satellites for $\Delta = 0.5$. The perfect step-like form assumed for $A(v)$ would even maintain this result in better approximations. One should, therefore, consider the experimental non-zero values at zero field of the second and fourth order satellites of phase 1/5 as a consequence of the deviations of the atomic modulations from a perfect step-like function.

In the cases of phases 2/9 and 2/11, an additional cause for non-zero even satellites at Δ=0.5 is the coherent overlap of (commensurate) satellites, disregarded above. For these two commensurate phases both even and odd order satellites superpose. This is not the case in phase 1/5. This is the reason for the significant higher value of I_2/I_3 in phases 2/9 and 2/11, compared with phase 1/5 (see Fig. 6). The second order satellite for phase 2/9 superposes terms m = 2,−7,11..., while in phase 2/11 the superposition involves m = 2,−9,13.... . As the amplitudes to be superposed decrease with 1/m, this also explains the higher value of I_2/I_3 for phase 2/9, compared to phase 2/11. One should take into account in this respect that the commensurate overlap correction is much weaker for I_3 in phases 2/9 and 2/11 as the two satellites of lower order to superpose are weak even-order satellites, which are zero in the ideal anti-symmetric step modulation.

4 Conclusions

The neutron diffraction experiments reported here evidence a polarization-flip transition under electric field of the five-fold phase (phase 1/5) of (full deuterated) BCCD. The polarization modulation along the c-axis approximately described by a chain of polar spins abruptly changes from a $\langle 5 \rangle$ configuration to a $\langle 64 \rangle$ one. This confirms the interpretation of earlier dielectric experiments [12]. The essential features and topology of the (E, T) phase diagram proposed in [12] concerning the competition between phases 2/9, 1/5 and 2/11 have also been confirmed. The threshold field at which the flip in the polarization configuration takes place is, however, considerably larger in our measurements (about 4 kV/cm higher). The deuteration of the samples of the present neutron experiments seems insufficient to explain this difference. Up to our knowledge BCCD is then the first experimental modulated system with competing periodicities where this type of field-induced polarization or spin flip transition is observed. Despite its plausibility, it has never been observed neither in other modulated ferroelectrics, nor in

modulated magnetic materials. Recently we have shown, however, using a simple general phenomenological model, that this type of phase transitions can be ubiquituous in polar modulated structures with saturated strong solitonic modulations [25].

Theoretical models for which this type of transitions occurs exhibit characteristic phase diagrams with self-similar features [22–24] and many multicritical points of very specific nature, the so-called upsilon points [24,28]. An upsilon point is an end point of a first-order transition line and an accumulation point of other upsilon points. Sasaki [24] has first pointed out the resemblance of the (E,T) phase diagram of BCCD to these theoretical ones and signaled BCCD as a first possible experimental system with upsilon points. The confirmation of a polarization flip transition in BCCD further supports this idea. In principle, this would imply the existence, between phases 2/9 and 1/5, in a very narrow temperature interval, of a cascade of higher-order commensurate phases (intermediate in the sense of the Farey tree hierarchy). Their transition lines would be essentially parallel in the (E,T) plane. A similar structure of transition lines would be present between phases 1/5 and 2/11. These intermediate phases have in general not been observed in the experiments above, but they cannot be discarded. Their temperature and electric field domains would be in principle so narrow that very accurate correlated tuning of temperature and electric field would be required to detect them. It is significant, in this respect, that the scans under 19.5 kV/cm, where field and temperature values were closer to the two hypothetical upsilon points limiting the horizontal flip transition line, the elastic scans exhibited a more complex structure (see Fig. 4), suggesting the presence of higher order commensurate phases. For instance, the scan represented in Figure 4 shows a small contribution of phase 3/14, which could be fitted quantitatively.

This work was supported in part by the UPV research grant 063.310-G19/98 and by the Spanish Ministry of Education grant PB98-0244. The authors are deeply indebted to J.M. Godard and to Mme Vaures (Laboratoire de Physique des Solides, Orsay, France) for the crystal elaboration, to Mme Lenain (LMDH, Université Pierre et Marie Curie, Paris, France) for the sample preparation, to P. Baroni and P. Boutrouille for technical assistance during the experiment at Orphée reactor (a special sample environmement was built to allow us to apply high electric field).

References

1. M.R. Chaves, in *Geometry and Thermodynamics*, edited by J.C. Tolédano (Plenum Press New York, 1990), pp. 353–369
2. G. Schaack, M. LeMaire, Ferroelectrics **208-209**, 1–62 (1998).
3. J.M. Perez-Mato, Solid State Commun. **32**, 933 (1979).
4. W. Selke, Phys. Rep. **170**, 213 (1998); J. Yeomans, Solid State Phys. **41**, 151 (1998).
5. J. Rossat-Mignod, P. Burlet, J. Villain, H. Bartholin, Wang Tcheng-Si, D. Florence, O. Vogt, Phys. Rev. B **16**, 440 (1977); J. von Boehm, P. Bak, Phys. Rev. Lett. **42**, 122 (1979).
6. R. Ao, G. Schaack, M. Schmitt, Zöller, Phys. Rev. Lett. **62**, 183 (1989); G. Schaack, M. Le Maire, Ferroelectrics **208-209**, 1 (1998).
7. B. Neubert, M. Pleimling, R. Siems, Ferroelectrics **208-209**, 141 (1998).
8. O. Hernandez, M. Quilichini, J.M. Perez-Mato, F.J. Zuniga, M. Dusek, J.M. Kiat, J.M. Ezpeleta, Phys. Rev. B **60**, 7025 (1999).
9. M.R. Chaves, A. Almeida, J.M. Kiat, W. Schwarz, J.C. Toledano, J. Schneck, A. Klöpperpieper, J. Albers, H.E. Müser, Phys. Rev. B **46**, 3098 (1992).
10. M.R. Chaves, A. Almeida, J.C. Toledano, J. Schneck, J.M. Kiat, W. Schwarz, J.L. Ribeiro, A. Klöpperpieper, J. Albers, H.E. Müser, Phys. Rev. B **48**, 13318 (1993).
11. O. Hernandez, J. Hlinka, M. Quilichini, Ferroelectrics **185**, 213 (1996).
12. M. Le Maire, R. Straub, G. Schaack, Phys. Rev. B **56**, 134 (1997).
13. I. Folkins, M.B. Walker, Z.Y. Chen, Phys. Rev. B **44**, 374 (1991).
14. D.G. Sannikov, G. Schaack, Phys. Rev. B **58**, 8313 (1998).
15. P. Rujan, W. Selke, G.V. Vimin, Z. Phys. B **53**, 221 (1983); W. Selke, P.M. Duxbury, Z. Phys. B **57**, 49 (1984).
16. C.S.O. Yokoi, Lei-Han Tang, Weiren Chou, Phys. Rev. B **37**, 2173 (1988).
17. S. Tanaka, M. Yamashita, J. Phys. Soc. Jpn **69**, 3339 (2000); S. Tanaka, M. Yamashita, Jpn J. Appl. Phys. **38**, L139 (1999); I. Harada, K. Takasaki, J. Phys. Soc. Jpn **54**, 2210 (1985).
18. J. Smith, J. Yeomans, J. Phys. C **16**, 5305 (1983).
19. A.M. Szpilka, J. Phys. C **18**, 569 (1985).
20. T. Janssen, in *Incommensurate Phases in Dielectrics. Fundamentals.* edited by R. Blinc, A.P. Levanyuk (North-Holland, 1986).
21. T. Honna, H. Amitsuka, S. Yasunami, K. Tenya, T. Sakakibara, H. Mitamura, T. Goto, G. Kido, S. Kawarazaki, Y. Miyako, K. Sugiyama, M. Date, J. Phys. Soc. Jpn **67**, 1017 (1998).
22. S. Aubry, F. Axel, F. Vallet, J. Phys. C **18**, 753 (1985).
23. N. Ishimura, J. Phys. Soc. Jpn **37**, 4752 (1985).
24. K. Sasaki, J. Phys. Soc. Jpn **68**, 3562 (1999).
25. J.M. Perez-Mato, I. Aramburu, M. Quilichini, S. Ivantchev, O. Hernandez, Phys. Rev. B **62**, 11 418 (2000).
26. J. Hlinka, M. Quilichini, R. Currat, J.F. Legrand, J. Phys. **8**, 8207 (1996); *ibidem* **8**, 8221 (1996); *ibidem* **9**, 1461 (1997).
27. J.M. Perez-Mato, G. Madariaga, F.J. Zúniga, A. Garcia Arribas, Acta Cryst. A **43**, 216 (1987); T; Janssen, A. Janner, A. Looijenga-Vos, P. de Wolf, *International Tables for Crystallography C*, edited by A.J.C. Wilson (Kluwer Academy Publishers, 1992), p. 797.
28. K.E. Bassler, K. Sasaki, R.B. Griffiths, J. Stat. Phys. **62**, 45 (1991).